HHS Public Access

Author manuscript

J Neurosci Res. Author manuscript; available in PMC 2019 January 07.

Published in final edited form as:

J Neurosci Res. 2013 May ; 91(5): 694–705. doi:10.1002/jnr.23200.

Valproic Acid Attenuates Microgliosis in Injured Spinal Cord and Purinergic $P2X_4$ Receptor Expression in Activated Microglia

Wen-Hsin Lu[#1], **Chih-Yen Wang**[#1], **Po-See Chen**[2], **Jing-Wen Wang**[1], **De-Maw Chuang**[3], **Chung-Shi Yang**[4,⋆], and **Shun-Fen Tzeng**[1,⋆]

[1]Department of Life Sciences, National Cheng Kung University, Tainan, Taiwan [2]Department of Psychiatry, College of Medicine, National Cheng Kung University, Tainan, Taiwan [3]Molecular Neurobiology Section, National Institute of Mental Health, National Institutes of Health, Bethesda, Maryland [4]Center for Nanomedicine Research, National Health Research Institutes, Zhunan, Taiwan

[#] These authors contributed equally to this work.

Abstract

Peripheral injection with a high dose of valproic acid (VPA), a histone deacetylase (HDAC) inhibitor, into animals with mild or moderate spinal cord injury (SCI) for 1 week can reduce spinal cord tissue loss and promote hindlimb locomotor recovery. A purinergic adenosine triphosphate (ATP) receptor subtype, $P2X_4$ receptor ($P2X_4R$), has been considered as a potential target to diminish SCI-associated inflammatory responses. In this study, using a minipump-based infusion system, we found that intraspinal infusion with VPA for 3 days into injured spinal cord significantly improved hindlimb locomotion of rats with severe SCI induced by a 10-g NYU impactor dropping from the height of 50 mm onto the spinal T9/10 segment. The neuronal fibers in the injured spinal cord tissues were significantly preserved in VPA-treated rats compared with those observed in vehicle-treated animals. Moreover, the accumulation of microglia/macrophages and astrocytes in the injured spinal cord was attenuated in the animal group receiving VPA infusion. VPA also significantly reduced $P2X_4R$ expression post-SCI. Furthermore, in vitro study indicated that VPA, but not the other HDAC inhibitors, sodium butyrate and trichostatin A (TSA), caused downregulation of $P2X_4R$ in microglia activated with lipopolysaccharide (LPS). Moreover, p38 mitogen-activated protein kinase (MAPK)-triggered signaling was involved in the effect of VPA on the inhibition of $P2X_4R$ gene expression. In addition to the findings from others, our results also provide important evidence to show the inhibitory effect of VPA on $P2X_4R$ expression in activated microglia, which may contribute to reduction of SCI-induced gliosis and subsequently preservation of spinal cord tissues.

Keywords

microglia; spinal cord injury; valproic acid; purinergic $P2X_4R$

[⋆] Correspondence to: Dr. Shun-Fen Tzeng, Department of Life Sciences, National Cheng Kung University, Tainan, Taiwan. stzeng@mail.ncku.edu.tw or Dr. Chung-hi Yang, Center for Nanomedicine Research, National Health Research Institutes, Zhunan Miaoli County, Taiwan. cyang@nhri.org.tw.

Spinal cord injury (SCI), which commonly results from traumatic episodes related to car accidents, gunshots, falls, or infections, can cause the loss of sensory or motor abilities. Primary SCI causes death of neurons, astrocytes, oligodendrocytes, and associated precursor cells as well as blood capillary damage. This destruction results in a series of pathological reactions known as secondary injuries; these include changes in blood vessels, hemorrhagic necrosis, inflammatory responses, and demyelination (Bareyre and Schwab, 2003; Deumens et al., 2005; Kerschensteiner et al., 2005). Moreover, many inflammatory cells such as T cells, macrophages, and microglia (CNS-resident macrophages) are recruited to the lesion to remove cell debris (Bareyre and Schwab, 2003). However, these inflammatory cells elicit excessive production of cytokines and chemokines, which causes secondary cell death, expansion of the lesion region, and functional impairment of the body (Bareyre and Schwab, 2003; Jones et al., 2005).

Valproic acid (VPA) is a simple, branched-chained fatty acid with anticonvulsant and mood stabilizer properties and works as a potent inhibitor of histone deacetylase (HDACs; Phiel et al., 2001). Notably, in vitro and in vivo studies have indicated that VPA acts as an anti-inflammatory and neuroprotective factor (Ichiyama et al., 2000; Li and El-Mallahk, 2000; Peng et al., 2005; Kim et al., 2007; Li et al., 2008; Biermann et al., 2010). VPA has been reported to stimulate the synthesis and release of neurotrophic factors in astrocytes and protects dopaminergic neurons from lipopolysaccharide (LPS)- or 1-methyl-4-phenylpyridinium (MPP^+)-induced neurotoxicity (Chen et al., 2006). Delayed transplantation of neural stem cells combined with VPA administration at 1 week postinjury has been reported to enhance hindlimb motor function in SCI mice, whereas delayed application of VPA alone showed no improvement in functional recovery (Abematsu et al., 2010). However, recent studies have indicated that intraperitoneal injection (i.p.) with a high dose of VPA for 1 week can reduce cell apoptosis via upregulation of neurotrophic factors, protective molecules, and matrix metalloprotease-9 (MMP-9), leading to enhanced locomotion recovery in moderate SCI rats (Lv et al., 2011a,b; Lee et al., 2012). Moreover, i.p. administration of VPA for weeks has been demonstrated to alleviate endoplasmic reticulum (ER) stress and oligodendrocytic cell death, which in turn induced better locomotor activity in moderate SCI (Penas et al., 2011).

High levels of adenosine triphosphate (ATP) released from damaged neurons and activated glia act as an excitotoxin in SCI and ischemia-associated inflammatory conditions (Wang et al., 2004; Di Virgilio et al., 2009). Extracellular ATP regulates the biological function of neural cells via its ionotropic P2X receptor (P2XR) and its G-protein-coupled metabotropic P2Y receptor (P2YR) subfamilies (Fields and Burnstock, 2006; Inoue et al., 2007). Among P2X receptor subtypes, $P2X_4R$ is known to play the regulatory role in tactile allodynia after peripheral nerve injury (Tsuda et al., 2005; Jarvis, 2009). Activation of this P2X subtype can trigger microglial activity and cytokine release (Inoue, 2006; Trang et al., 2006, 2009). $P2X_4R$ also plays a critical role in inflammation and the development of neuropathic pain in the spinal cord (Tsuda et al., 2003; Inoue, 2006; Cotrina and Nedergaard, 2009). In addition, persistent accumulation of cells expressing $P2X_4R$ is observed at the lesion site after SCI (Schwab et al., 2005). The main population of the $P2X_4R$-expressing cells in the lesion center (LC) has been identified as activated microglia/macrophages (Schwab et al., 2005).

Recently, it has been shown that deficiency of $P2X_4R$ leads to reduction of interleukin-1β (IL-1β) levels and attenuating the infiltration of neutrophils and macrophages after SCI, pointing to $P2X_4R$ as a potential therapeutic target for SCI and other neurodegenerative diseases (de Rivero Vaccari et al., 2012).

Evidence indicates that the plasma elimination half-life of VPA is 2.3–4.6 hr in rats receiving i.p. or i.v. administration (Loscher, 1978; Binkerd et al., 1988). Because of the short half-life, the repeated i.p. administration of VPA at high doses is often adopted. Clinical data have shown that the side effects of VPA include nausea, vomiting, gastrointestinal distress, and weight gain (Dreifuss et al., 1987; Biton et al., 2001; Chengappa et al., 2002). Thus, in this study, a 3-day minipump-based infusion system was used to evaluate the efficacy of a short-term treatment with VPA at the low dosage for spinal cord repair. We found that VPA infusion not only increased the remaining neuronal fibers but also reduced $P2X_4R$ expression and gliosis in the injured spinal cord. Moreover, in vitro study showed that the addition of VPA downregulated TNF-α mRNA expression and reduced $P2X_4R$ expression in LPS-activated microglia through p38MAPK signaling pathway. These effects could contribute to hindlimb locomotion recovery in rats with severe SCI.

MATERIALS AND METHODS

Animals, Spinal Cord Injury Surgery, and VPA Infusion

SCI was induced with a weight-drop device developed at New York University (Constantini and Young, 1994; Basso et al., 1995) and was performed as reported previously (Cheng et al., 2002). Female adult Sprague-Dawley rats (n = 41; 250 ± 30 g; BioLasco Taiwan Corporation, Taipei, Taiwan) were anesthetized with pentobarbital (50 mg/kg, i.p.), and the spinal cord was exposed by laminectomy at the level of T9/T10. A 10-g rod was dropped onto the laminectomized cord from a height of 50 mm to induce SCI. To evaluate the efficacy of continuous VPA infusion, an Alzet osmotic pump (model 1003D; Durect, Cupertino, CA) with a delivery rate of 1.0 μl/hr and a 3-day duration was applied. The osmotic pump was prefilled with 1.5 μg VPA (n = 17) or PBS (n = 15), connected to the infusion cannula with a Brain Infusion Kit III (Durect), and primed for 2 hr in saline at 37°C. Five to ten minutes after SCI, the osmotic pump containing VPA or PBS (vehicle) was placed slightly proximal to the LC and about 0.7–0.8 mm below the dura (Wang et al., 2008). The sham group of rats underwent T9 laminectomy without weight-drop injury and displayed normal hindlimb locomotion after surgery. During surgery, rectal temperature was maintained at 37°C with a thermostatically regulated heating pad. Bladder evacuation was applied on a daily basis. Antibiotic treatment using sodium ampicillin (Pfizer, Taipei, Taiwan) at a dose of 80 mg/kg was injected for 1 week after injury. Animal surgery and care were provided in accordance with the Laboratory Animal Welfare Act and NIH *Guide for the care and use of laboratory animals* and were approved by the Institutional Animal Care and Use Committee of National Cheng Kung University (Taiwan).

Behavioral Analysis

Animals receiving either vehicle or VPA were assessed for locomotor function by two blinded observers, using the BBB hindlimb locomotor rating scale (Basso et al., 1996). Locomotor activities were evaluated by placing animals in an open field apparatus with a molded plastic surface for 4 min. Hindlimb locomotor recovery in animals was scored on a scale of 0–21. The analysis was performed every 2–3 days for 1 month on specified days (days 3, 5, 7, 9, 12, 14, 16, 18, 21, and 31 post-SCI). A score of 0 indicated that hindlimb locomotion ability was totally lost, whereas a score of 21 indicated normal hind limb locomotion ability.

Histological Staining

Experimental animals were perfused intracardially with 0.9% ice-cold NaCl, followed by 4% paraformaldehyde in 0.1 M PBS. Spinal cord tissues were removed, postfixed in 4% paraformaldehyde overnight, and cryoprotected in 30% (w/v) sucrose in PBS for 2–3 days. The cords (approximately 2 cm in length containing the LC) were embedded in Tissue Tek OCT (Electron Microscopy Sciences, Fort Washington, PA), and then horizontal tissue sections with a 14-μm thickness/section were made with a Cryostat (Leica). Cryostat tissue sections were rinsed with PBS and then incubated with 0.1% cresyl violet solution (with 0.3% acetic acid) at 37°C for 10 min. After a quick rinse in distilled water, tissue sections were dehydrated in 95% and 100% ethanol. Slides were cleared with xylene and mounted in Entellan.

Immunohistochemistry

The horizontal (or transverse) tissue sections with a 14-μm thickness were incubated in PBS containing 0.1% Triton X-100 for 30 min, and then treated with primary antibodies in PBS plus 5% horse serum overnight at 4°C. After removal of primary antibodies by washing with PBS, biotinylated secondary antibodies (Vector, Burlingame, CA) were added and incubated for 1 hr at room temperature. Slides were incubated under dark conditions with fluorescein isothiocyanate (FITC)-avidin D (Vector) for 45 min at room temperature and then were mounted using 90% glycerol. The primary antibodies used in this study included rabbit anti-GFAP (Chemicon, Temecula, CA), rabbit anti-NF-200 (Sigma-Aldrich, St. Louis, MO), rabbit anti-Iba1 (Wako Pure Chemical, Osaka, Japan), and rabbit anti-$P2X_4R$ (Alomone Labs, Jerusalem, Israel).

Quantification of $NF200^+$ Neuronal Fibers and Microglia

$NF200^+$ neuronal fiber and $Iba1^+$ microglia quantification was performed by counting $NF200^+$ fibers or $Iba1^+$ cells in five randomly sampled images captured from each spinal cord tissue using an epifluorescence microscope under ×10 objective in Imaging J analysis software (NIH). The total neuronal fibers per section and the average neuronal fibers with distinct lengths (less than 25, 50, and 100 μm or greater than 100 μm) per section were measured (three animals in each vehicle-treated group or VPA-treated group). The values were obtained by calculating the ratio of average $Iba1^+$ cell number per field in VPA-treated spinal cord vs. total $Iba1^+$ cells in each field from the spinal cord section of vehicle-operated group.

Double Immunofluorescence

Cryostat tissue sections were permeabilized with 0.1% Triton X-100 for 30 min and incubated overnight with rabbit anti-$P2X_4R$ antibody at 4°C. On the following day, the antibody was washed off, and the sections were incubated with the CFL-594-labeled secondary antibody (Santa Cruz Biotechnology, Santa Cruz, CA) for 1 hr. Subsequently, goat anti-Iba1 (Abcam, Cambridge, MA) was applied at room temperature for 3 hr. The tissue sections were then incubated with the biotinylated secondary antibody (Vector) for 1 hr, followed by FITC-avidin D (Vector) for 45 min. After being washed, the sections were mounted in 90% glycerol.

Western Blotting

The spinal segment, 3–4 mm in length, containing the LC of SCI rats was stored in liquid nitrogen overnight and homogenized using a disposable grinding stick. Tissue blocks were homogenized in lysis buffer containing 50 mM Tris-HCl (pH 7.5), 250 mM NaCl, 5% NP-40, and protease inhibitor cocktail (Sigma). Protein concentration was determined using the Bio-Rad DC kit (Bio-Rad, Hercules, CA). Protein extracts (50 μg/lane) were separated by 10% SDS-PAGE and then transferred to a nitrocellulose filter (Millipore, Billerica, MA). The membrane was probed overnight at 4°C with primary antibodies at an appropriate dilution, and then incubated with horseradish peroxidase (HRP)-conjugated secondary antibodies (Jackson Immunoresearch, West Grove, PA) for 1 hr at room temperature. Detection was conducted by ECL chemiluminescence (Amersham Pharmacia, Buckinghamshire, United Kingdom). Primary antibodies used for the study were as follows: rabbit anti-GFAP, rabbit anti-$P2X_4R$, rabbit anti-p38MAPK, rabbit antiphosphop38MAPK (Cell Signaling, Danvers, MA), rabbit anti-Mn-SOD (Assay Designs, Ann Arbor, MI), anti-catalase (Abcam), mouse anti-actin regulatory protein (CAPG; Santa Cruz Biotechnology), mouse anti-β-actin (Santa Cruz Biotechnology), and mouse anti-glyceraldehyde 3-phosphate dehydrogenase (GAPDH; Chemicon),

Primary Microglial Culture

Microglia isolated from cerebral cortices of neonatal Sprague-Dawley rat brains (P2–3) were cultured as described previously (Fang et al., 2009). After centrifugation, the cells (10^7 cells/flask) were plated onto poly-D-lysine (PDL; Sigma-Aldrich)-coated 75-cm^2 tissue culture flasks with DMEM/F12 medium (Invitrogen, Carlsbad, CA) containing 10% fetal bovine serum (FBS; Hyclone, Logan, UT), 50 U/ml penicillin, and 50 mg/ml streptomycin (Invitrogen). The medium was replaced every 2–3 days. Eight days later, primary rat microglia were collected using the shake-off method (McCarthy and de Vellis, 1980). The cells were replated and treated with VPA in DMEM/F12 medium containing N1 serum supplement. In general, 95% of cells in the culture consisted of primary rat microglia with B4-isolectin positive staining; less than 5% of cells were found to be $GFAP^+$ astrocytes. Microglia were replated onto 60-mm tissue Petri dishes at a density of 5×10^5 cells per dish and then treated with VPA in the presence of LPS (Sigma).

Quantitative Real-Time PCR

Total RNA was isolated from injured spinal cord tissues of SCI rats or cultured microglia using Trizol reagent (Invitrogen). One microgram of total RNA was then used for reverse transcription reaction with MMLV-reverse transcriptase, and Q-PCR was performed as previously described (Fang et al., 2009). Q-PCR assay for the expression of rat $P2X_4R$ or tumor necrosis factor-α (TNF-α) mRNA was accessed with a Roche LightCycler using LightCycler FastStart DNA Master SYBR Green I kit (Roche, Indianapolis, IN). PCR amplification of $P2X_4R$ or TNF-α was performed for 10 min at 95°C, followed by 50 cycles set for 10 sec each at 95°C, annealing for 10 sec at 60°C, and extension for 20 sec at 72°C. The results were normalized to cyclophilin A (CyPA) and expressed as a ratio of $P2X_4R$ or TNF-α to the CyPA control. The specific primers were designed for $P2X_4R$, TNF-α, and CyPA using LightCycler Probe Design Software 2 (Roche Diagnostics, Mannheim, Germany) and synthesized by MWG Biotech AG (Ebersberg, Germany). Polymerase chain reactants were also analyzed on 1% agarose gels to confirm primer specificity by observing the purity of single PCR products during amplification. The specific primer sequences for rat $P2X_4R$ and TNF-α are as follows: $P2X_4R$ (NM_031594) primers, 5′-AGACGTTCTTCC ACC CTAT-3′ (forward), 5′-CTCTCAGACCCTTC CTACC-3′ (reverse); TNF-α (NM_012675) primers, 5′-TCTCAAAACT CGAGTGACAAG-3′ (forward), 5′-AGTTGGTTGTCTTT GAGATCC-3′ (reverse).

Statistical Analysis

The results are presented as mean ± SEM. Two-tailed unpaired Student's *t*-test and two-way ANOVA for BBB behavioral analysis were performed to evaluate statistical significance ($^{\star}P < 0.05$, $^{\star\star}P < 0.01$).

RESULTS

Effect of VPA on Hindlimb Locomotion in Rats With SCI

Many immediate-early genes, most of which are inflammation related, are upregulated during the first 6 hr post-SCI (Carmel et al., 2001; Song et al., 2001; Pan et al., 2002). Moreover, the spectrum of the gene expression changes between the first 12 hr and the third day after SCI revealed the occurrence of both cell survival and degeneration/cell death during this interval (Grossman et al., 2001; Song et al., 2001). Here we conducted intraspinal implantation of an osmotic pump loading VPA solution into the injured spinal cord commencing immediately after SCI (Fig. 1A). The sustained infusion of VPA was performed at a rate of 500 ng/day for the first 3 days post-SCI. Hindlimb locomotion of experimental rats was assessed at indicated days using BBB score analysis in an open field test. Results demonstrated that SCI rats receiving a 3-day infusion of VPA showed progressive improvement on BBB scores (Fig. 1B). Notably, at week 3, BBB scores in rats receiving VPA infusion dramatically increased to 8.38 ± 0.18. By day 31 post-SCI, locomotor function in VPA-treated rats showed continuous improvement with increased BBB scores (10.63 ± 0.42). BBB scores in vehicle-treated animals remained low (approximately 2.17 at days 21 and 31) for the entire period. Histological examination showed that more preserved tissues were observed in the LC of the VPA-treated group compared with that found in the vehicle-treated animals (Fig. 1C). To examine the remaining

neuronal fibers in the injured spinal cord at day 31 post-SCI, we performed immunofluorescence staining for NF-200 on SCI rats receiving continuous infusion of VPA or vehicle. The remaining elongated NF-200$^+$ neuronal fibers with length greater than 25 μm were increased in the LC of the spinal cord in those rats treated with a 3-day infusion of VPA (Fig. 1D, arrows, and E) compared with that in the vehicle-treated control (Fig. 1E). Moreover, NF-200$^+$ debris was observed in the LC of vehicle-treated spinal cord (Fig. 1D, arrowheads). The NF-200$^+$ fibers in the injured spinal cord at the LC of VPA-treated spinal cord were preserved in the VPA-receiving group compared with the vehicle-treated group (Fig. 1F). These data show that continuous infusion with VPA for 3 days preserved the neuronal fibers to some extent in the lesion site of the spinal cord after chronic SCI and facilitated the improved hindlimb locomotor performance in rats with severe SCI.

Reduction of Microglia/Macrophages Accumulated in the Injured Spinal Cord Tissue by 3-Day Infusion of VPA

The anti-inflammatory properties of VPA in the inflamed CNS are based on its ability to reduce microglia and immune cells (Peng et al., 2005; Kim et al., 2007). Using immunofluorescence for Iba1, a marker of resting and activated microglia/macrophages, the accumulation of Iba1$^+$ microglia/macrophages with an amoeboid shape was observed in the injured spinal cord proximal to the LC of the vehicle-treated spinal cord at day 31 (Fig. 2A). Moreover, Iba1$^+$ microglia accumulated in the remaining tissues surrounding the cavity displayed an active amoeboid shape (Fig. 2B,D,J,L). Iba1$^+$ cells observed in the lateral part of the spinal cord showed a hypertrophic form with the processes (Fig. 2C,K, arrows). Iba1 immunoreactivity was also seen in the injured spinal cord of VPA-treated animals (Fig. 2E). However, tissue debris immunoreactive for Iba1 was observed in the injured tissue surrounding the cavity of VPA-treated animals (Fig. 2F,M, arrowhead). Moreover, Iba1$^+$ cells found in the lateral portion of the injured spinal cord (Fig. 2G,H) showed a hypotrophic shape (Fig. 2N,O). The quantitative results showed that Iba1$^+$ microglia/macrophages in the injured spinal cord were significantly reduced in VPA-infused spinal cord compared with that found in the vehicle-treated spinal cord (Fig. 2I). Previously, we have reported that β-actin$^+$ immune cells accumulated in the LC post-SCI and that high levels of actin regulatory proteins (CAPG) were detected in the LC at day 14 post-SCI (Wang et al., 2011). Moreover, this was associated with a decline in catalase and Mn-superoxide dismutase (Mn-SOD) in the LC (Wang et al., 2011). Therefore, we examined the levels of these four proteins in the LC of VPA-treated spinal cord. VPA infusion reduced β-actin and CAPG levels at the LC (Fig. 3A). Moreover, the levels of catalase and Mn-SOD at the LC were significantly increased by VPA infusion compared with the vehicle-treated control group (Fig. 3B). These observations suggest that the accumulation of immune cells in the lesion center was attenuated by VPA infusion. Moreover, treatment with VPA increased endogenous antioxidant enzymes in the injured spinal cord.

GFAP immunostaining was also performed to examine the effect of VPA infusion on astrocyte reactivity. GFAP$^+$ astrocytes were largely accumulated within the region surrounding the lesion cavity located at the dorsal cord portion of the vehicle-treated (Fig. 4A–D) and VPA-infused rats (Fig. 4F). Hypertrophic GFAP^1 astrocytes were observed in the ventral–lateral areas of the vehicle-treated spinal cord tissue (Fig. 4C,D, arrows), whereas

hypotrophic GFAP$^+$ astrocytes were found in the lateral portion of VPA-treated spinal cord tissue (Fig. 4G,H, arrowheads). In addition, a reduced level of GFAP was detected at the VPA-infused lesion site of the spinal cord compared with that found in the vehicle-treated spinal cord (Fig. 4I). The observations reveal that VPA infusion could alleviate glial reactivity in the injured spinal cord.

Downregulation of P2X$_4$R Expression With the Addition of VPA

The upregulation of P2X$_4$R is known to be associated with the activation of microglia/macrophages in the damaged/inflamed spinal cord (Schwab et al., 2005). Moreover, P2X$_4$R has been indicated to serve as the therapeutic target for SCI-associated or other neurodegenerative diseases (de Rivero Vaccari et al., 2012). Therefore, we further examined the time profile of expression of P2X$_4$R at the LC or in the spinal cord 0.5–1.0 cm rostral (r0.5 and r1) and caudal (c0.5 and c1) to the LC at days 1, 7, and 14 post-SCI. Results indicated that P2X$_4$R mRNA levels were dramatically increased in the injured spinal cord tissue, including the LC, regions rostral (r0.5 and r1) to the LC, and regions caudal (c0.5 and c1) to the LC at days 7 and 14 post-SCI (Fig. 5A). Moreover, the P2X$_4$R-immunostained cells were colocalized to Iba1$^+$ amoeboid microglia/macrophages in the dorsal and ventral portions of the spinal cord proximal to the LC at day 7 post-SCI (Fig. 5B). No P2X$_4$R-expressing cells were observed in the lateral area of sham-operated spinal cord tissues (Fig. 5B) or other spinal cord regions (data not shown). Our results showing increased expression profile of P2X$_4$R in the injured spinal cord indicate that P2X$_4$R upregulation was associated with SCI-associated microglia activation.

Accordingly, we conducted in vivo experiments by intraspinal infusion of VPA at a rate of 500 ng/day commencing immediately after SCI using an osmotic pump for the first 3 days post-SCI (Fig. 6A). At day 14 post-SCI, the spinal cord tissues were removed and subjected to Q-PCR for P2X$_4$R mRNA expression. As shown in Figure 6A, P2X$_4$R mRNA expression in the LC and injured spinal cord 5 mm caudal to the LC (c0.5) was robustly downregulated by a 3-day infusion with VPA compared with the vehicle-treated control (Fig. 6B). Moreover, P2X$_4$R protein levels in the LC of the VPA-treated group had significantly declined at day 7 post-SCI (Fig. 6C). The in vivo observations reveal that the VPA-induced reduction of P2X$_4$R levels in the injured spinal cord provides evidence for a role of VPA in spinal cord repair.

Downregulation of P2X$_4$R Expression in Cultured Microglia With Exposure of VPA

Given our in vivo results, we asked whether direct application of VPA into the damaged spinal cord tissues inhibited P2X$_4$R expression in activated microglia. To evaluate whether VPA might exert the regulatory effect on P2X$_4$R mRNA expression in activated microglia, we performed in vitro studies using primary rat microglia activated by 10 ng/ml the endotoxin LPS. The morphological examination indicated that exposure to VPA caused no significant change in the morphology of LPS-stimulated microglia (Fig. 7A) or in their cell viability (data not shown). Similarly to the findings from others (Peng et al., 2005; Chen et al., 2007), we found that the addition of VPA attenuated TNF-α mRNA expression in LPS-stimulated microglia (Fig. 7D). Furthermore, we examined the effect of VPA on P2X$_4$R expression in LPS-activated microglia. By Q-PCR analysis, P2X$_4$R mRNA levels in LPS-

stimulated microglia were reduced by exposure to VPA for 18 hr (Fig. 7B). In contrast to the VPA effect, other HDAC inhibitors, sodium butyrate and TSA, significantly increased $P2X_4R$ mRNA expression in LPS-activated microglia (Fig. 7C) as well as TNF-α mRNA expression (Fig. 7E). Note that the three HDACs were able to increase the levels of acetylated H3 in LPS-activated microglia (data not shown). The results suggest that VPA-induced inhibition of $P2X_4R$ mRNA expression might be not occured through HDAC inhibitory action. VPA addition also inhibits TNF-α production in LPS-stimulated microglia.

VPA has been reported to induce cell apoptosis of LPS-untreated mouse microglia through the activation of p38MAPK (Xie et al., 2010). Western blot analysis indicated that the phosphorylation of p38MAPK in LPS-activated microglia was significantly increased at 10 min after VPA addition compared with that in the control (Fig. 8A). Decline in the phosphorylation of p38MAPK was observed at 30 min after exposure of LPS-activated microglia to VPA. Therefore, we next examined whether the inhibitor of p38MAPK SB203580 can block the VPA-induced inhibitory effect on TNF-α mRNA expression in LPS-stimulated microglia. Pretreatment with the p38MAPK inhibitor SB203580 significantly blocked VPA-induced inhibition of TNF-α mRNA expression in LPS-stimulated microglia (Fig. 8B). The results indicate that pretreatment with SB203580 significantly blocked the inhibitory effect of VPA on $P2X_4R$ mRNA expression of LPS-stimulated microglia (Fig. 8C), suggesting that VPA-induced downregulation of $P2X_4R$ expression in LPS-activated microglia occurred through the p38MAPK-dependent signal pathway.

DISCUSSION

Here we describe two major findings. First, intraspinal infusion with VPA for 3 days effectively reduces $P2X_4R$ levels in the LC of the spinal cord derived from rats with SCI, along with an increased level of antioxidant enzymes (catalase and Mn-SOD) and a decline in SCI-associated gliosis. Second, the direct application of VPA onto LPS-stimulated microglia cultures caused significant reduction in $P2X_4R$ mRNA expression in activated microglia. The effect of VPA was mediated by the induction of p38MAPK activation but not through its action on the inhibition of HDAC. These observations indicate that VPA has an effect on the inhibition of $P2X_4R$ expression in activated microglia could contribute to the alleviation of gliosis occurring after SCI and promote hindlimb locomotion in rats with SCI.

Given the fact that increased inflammatory mediators, apoptotic cell death, and reactive gliosis were observed during the first 3 days after SCI (Schnell et al., 1999; Bethea and Dietrich, 2002), we performed continuous VPA delivery to the lesion site at a controlled rate, using an osmotic pump for 3 days to maintain availability. Indeed, our findings indicate that better hindlimb locomotor recovery was induced by 3 days of continuous VPA infusion after SCI. We have recently reported that increased levels of structurally related proteins, specifically, β-actin and CAPG, at the LC on days 7 and 14 post-SCI could result from the substantial accumulation of inflammatory cells at the LC. This is associated with a decline of Mn-SOD and catalase protein levels in the LC of the injured spinal cord (Wang et al., 2011). We show here that VPA infusion significantly increased levels of Mn-SOD and

catalase, accompanied by the reduction of β-actin and CAPG levels in the LC of VPA-treated animals at day 7 post-SCI. Our in vivo experiments further demonstrated that the number of $Iba1^+$ amoeboid microglia/macrophages and glial scar formation were eliminated in the injured spinal cord of rats receiving VPA infusion. The findings demonstrate that the alleviation of inflammatory cells might derive from increased neural cell survival in the rats receiving osmotic VPA infusion. This could in turn reduce secondary tissue damage following the primary impact on the spinal cord tissue. Our findings are also consistent with observations from others showing that inflammation and activated macrophages/microglial cells in the lesion site of severe SCI were reduced by i.p. VPA injection for 7 days (Abdanipour et al., 2012; Yu et al., 2012).

Recent findings have demonstrated that $P2X_4R$ gene deficiency leads to reduced IL-1β levels and attenuated infiltration of neutrophils and macrophages after SCI (de Rivero Vaccari et al., 2012), pointing to $P2X_4R$ as a potential therapeutic target for SCI and other neurodegenerative diseases. The $P2X_4R$-induced intracellular signaling pathway triggers microglial activation in response to immune stimuli (Mingam et al., 2008; Monif et al., 2009) and exacerbates neuronal loss and cell death (Bernardino et al., 2008). Schwab and his coworkers (2005) have reported that $P2X_4R^+$ cells accumulated greatly in the traumatic epicenter at 24 hr post-SCI, reaching maximal levels at day 7. Persistent accumulation of $P2X_4R^+$ cells was still observed at week 4 after SCI. Similarly to the previous observations from Schwab et al., we observed that $P2X_4R^+$ cells colocalized with $IbaI^+$ amoeboid microglia/macrophages were highly present in the epicenter of the injured spinal cord post-SCI. Moreover, SCI-induced increases in $P2X_4R$ mRNA levels were detected in the injured spinal cord throughout the rostral portions, LC, and caudal regions at days 7 and 14 after severe SCI. The results indicate that $P2X_4R$ upregulation in the injured spinal cord was associated with activation of microglia/macrophages in the LC. Furthermore, our results show that VPA reduced levels of $P2X_4R$ and $Iba1^+$ microglia in the lesioned spinal cord, indicating that VPA may suppress SCI-induced activation of macrophages and microglia. This could also occur because infusion with VPA prevents spinal neural cells from blunt trauma-induced injury; therefore, less neural death would induce a milder inflammatory reaction in the LC. That is, the lowered $P2X_4R$ expression may result from the downregulation of activated microglia/macrophages in the injured spinal cords of rats receiving VPA. However, it is also possible that VPA continuously infused into the LC acted on activated microglia and attenuated $P2X_4R$ mRNA expression, which in turn suppressed microglia/ macrophage activation. This possibility is supported by the recent findings that VPA did not induce human microglia apoptosis but reduced human microglial dysfunction (Gibbons et al., 2011).

VPA and other HDAC inhibitors have been considered as potential neuroprotective drugs via the inhibition of HDAC causing hyperacetylation (Chuang et al., 2009). The VPA analog sodium butyrate and the structurally unrelated TSA have been reported to induce the cell death of microglia without LPS activation (Chen et al., 2007). In contrast to the VPA effect on downregulation of $P2X_4R$ expression in LPS-stimulated microglia, the study described here indicates that sodium butyrate and TSA induced significant upregulation of $P2X_4R$ mRNA expression in LPS-stimulated microglia. Similarly to the findings from others with pre-exposure of LPS-activated microglia to VPA (Peng et al., 2005), we have found that

posttreatment with VPA, but not sodium butyrate and TSA, significantly reduced TNF-α mRNA expression in LPS-stimulated microglia. It has been reported that sodium butyrate effectively reduced interferon-γ mediated TNF-α production but not LPS-mediated TNF-α expression (Kim et al., 2004). Moreover, TSA has been found to enhance LPS-mediated nuclear factor-κB signaling, which promoted the expression of its target genes, such as TNF-α (Park et al., 2005). In conjunction with our findings regarding their effect on increased expression of $P2X_4R$ and TNF-α mRNA levels, sodium butyrate and TSA might drive LPS-stimulated microglia toward the more active state. Together, the mechanism responsible for VPA-reduced expression of $P2X_4R$ expression in LPS-activated microglia is distinct from that triggered by sodium butyrate and TSA. Thus, VPA-induced inhibition of $P2X_4R$ mRNA expression is less likely via the inhibition of HDAC.

VPA allows induction of the p38MAPK signaling in the mouse BV2 cell line and mouse primary microglia without LPS activation, resulting in cell apoptosis (Xie et al., 2010). Our findings here shown that exposure to VPA significantly increased the phosphorylation of p38MAPK in rat primary microglia activated by LPS, whereas VPA addition only slightly changed phosphorylated p38MAPK levels in rat microglia without LPS stimulation (data not shown). These results indicate that VPA rapidly triggered p38MAPK activation in LPS-stimulated microglia. Furthermore, treatment of LPS-activated microglia with the p38MAPK inhibitor prior to VPA addition effectively blocked the inhibitory effect of VPA on microglial $P2X_4R$ mRNA expression, suggesting that VPA downregulated $P2X_4R$ mRNA expression via p38MAPK signaling.

In conclusion, our study demonstrates that continuous intraspinal VPA infusion for 3 days after acute SCI markedly alleviated $P2X_4R$ expression and gliosis in the injured spinal cord tissue. The action of VPA on the inhibition of glial reactivity contributes to better locomotor activity in rats with severe SCI. Overall, in conjunction with in vitro data showing VPA-induced inhibition of $P2X_4R$ expression in activated microglia, our results support the potential usefulness of intraspinal VPA administration in treating SCI as well as $P2X_4R$-associated neuropathogenesis.

ACKNOWLEDGMENTS

The authors thank Dr. Jen-Kun Chen and Ms. Yi-Ting Wu (Center for Nanomedicine Research, National Health Research Institutes, Zhunan, Taiwan) for their excellent technical instruction and assistance.

Contract grant sponsor: National Science Council of Taiwan; Contract grant number: NSC 98–2321-B-006–002; Contract grant number: NSC 99–2321-B-006–002.

REFERENCES

Abdanipour A, Schluesener HJ, Taki T. 2012 Effects of valproic acid, a histone deacetylase inhibitor, on improvement of locomotor function in rat spinal cord injury based on epigenetic science. Iranian Biomed J 16:90–100.

Abematsu M, Tsujimura K, Yamano M, Saito M, Kohno K, Kohyama J, Namihira M, Komiya S, Nakashima K. 2010 Neurons derived from transplanted neural stem cells restore disrupted neuronal circuitry in a mouse model of spinal cord injury. J Clin Invest 120:3255–3266. [PubMed: 20714104]

Bareyre FM, Schwab ME. 2003 Inflammation, degeneration and regeneration in the injured spinal cord: insights from DNA microarrays. Trends Neurosci 26:555–563. [PubMed: 14522149]

Basso DM, Beattie MS, Bresnahan JC. 1995 A sensitive and reliable locomotor rating scale for open field testing in rats. J Neurotrauma 12:1–21. [PubMed: 7783230]

Basso DM, Beattie MS, Bresnahan JC, Anderson DK, Faden AI, Gruner JA, Holford TR, Hsu CY, Noble LJ, Nockels R, Perot PL, Salzman SK, Young W. 1996 MASCIS evaluation of open field locomotor scores: effects of experience and teamwork on reliability. Multicenter Animal Spinal Cord Injury Study. J Neurotrauma 13:343–359. [PubMed: 8863191]

Bernardino L, Balosso S, Ravizza T, Marchi N, Ku G, Randle JC, Malva JO, Vezzani A. 2008 Inflammatory events in hippocampal slice cultures prime neuronal susceptibility to excitotoxic injury: a crucial role of $P2X_7$ receptor-mediated IL-1beta release. J Neurochem 106:271–280. [PubMed: 18384650]

Bethea JR, Dietrich WD. 2002 Targeting the host inflammatory response in traumatic spinal cord injury. Curr Opin Neurol 15:355–360. [PubMed: 12045737]

Biermann J, Grieshaber P, Goebel U, Martin G, Thanos S, Di Giovanni S, Lagreze WA. 2010 Valproic acid-mediated neuroprotection and regeneration in injured retinal ganglion cells. Invest Ophthalmol Vis Sci51:526–534.

Binkerd PE, Rowland JM, Nau H, Hendrickx AG. 1988 Evaluation of valproic acid (VPA) developmental toxicity and pharmacokinetics in Sprague-Dawley rats. Fundam Appl Toxicol 11:485–493. [PubMed: 3146521]

Biton V, Mirza W, Montouris G, Vuong A, Hammer AE, Barrett PS. 2001 Weight change associated with valproate and lamotrigine monotherapy in patients with epilepsy. Neurology 56:172–177. [PubMed: 11160951]

Carmel JB, Galante A, Soteropoulos P, Tolias P, Recce M, Young W, Hart RP. 2001 Gene expression profiling of acute spinal cord injury reveals spreading inflammatory signals and neuron loss. Physiol Genomics 7:201–213. [PubMed: 11773606]

Chen PS, Peng GS, Li G, Yang S, Wu X, Wang CC, Wilson B, Lu RB, Gean PW, Chuang DM, Hong JS. 2006 Valproate protects dopaminergic neurons in midbrain neuron/glia cultures by stimulating the release of neurotrophic factors from astrocytes. Mol Psychiatry 11:1116–1125. [PubMed: 16969367]

Chen PS, Wang CC, Bortner CD, Peng GS, Wu X, Pang H, Lu RB, Gean PW, Chuang DM, Hong JS. 2007 Valproic acid and other histone deacetylase inhibitors induce microglial apoptosis and attenuate lipopolysaccharide-induced dopaminergic neurotoxicity. Neuroscience 149:203–212. [PubMed: 17850978]

Cheng H, Wu JP, Tzeng SF. 2002 Neuroprotection of glial cell line-derived neurotrophic factor in damaged spinal cords following contusive injury. J Neurosci Res 69:397–405. [PubMed: 12125080]

Chengappa KN, Chalasani L, Brar JS, Parepally H, Houck P, Levine J. 2002 Changes in body weight and body mass index among psychiatric patients receiving lithium, valproate, or topiramate: an open-label, non-randomized chart review. Clin Ther 24:1576–1584. [PubMed: 12462287]

Chuang DM, Leng Y, Marinova Z, Kim HJ, Chiu CT. 2009 Multiple roles of HDAC inhibition in neurodegenerative conditions. Trends Neurosci 32:591–601. [PubMed: 19775759]

Constantini S, Young W. 1994 The effects of methylprednisolone and the ganglioside GM1 on acute spinal cord injury in rats. J Neurosurg 80:97–111. [PubMed: 8271028]

Cotrina ML, Nedergaard M. 2009 Physiological and pathological functions of $P2X_7$ receptor in the spinal cord. Purinergic Signalling 5:223–232. [PubMed: 19205927]

de Rivero Vaccari JP, Bastien D, Yurcisin G, Pineau I, Dietrich WD, De Koninck Y, Keane RW, Lacroix S. 2012 $P2X_4$ receptors influence inflammasome activation after spinal cord injury. J Neurosci 32:3058–3066. [PubMed: 22378878]

Deumens R, Koopmans GC, Joosten EA. 2005 Regeneration of descending axon tracts after spinal cord injury. Prog Neurobiol 77:57–89. [PubMed: 16271433]

Di Virgilio F, Ceruti S, Bramanti P, Abbracchio MP. 2009 Purinergic signalling in inflammation of the central nervous system. Trends Neurosci 32:79–87. [PubMed: 19135728]

Dreifuss FE, Santilli N, Langer DH, Sweeney KP, Moline KA, Menander KB. 1987 Valproic acid hepatic fatalities: a retrospective review. Neurology 37:379–385. [PubMed: 3102998]

Fang KM, Yang CS, Sun SH, Tzeng SF. 2009 Microglial phagocytosis attenuated by short-term exposure to exogenous ATP through P2X receptor action. J Neurochem 111:1225–1237. [PubMed: 19860838]

Fields RD, Burnstock G. 2006 Purinergic signalling in neuron–glia interactions. Nat Rev Neurosci 7:423–436. [PubMed: 16715052]

Gibbons HM, Smith AM, Teoh HH, Bergin PM, Mee EW, Faull RL, Dragunow M. 2011 Valproic acid induces microglial dysfunction, not apoptosis, in human glial cultures. Neurobiol Dis 41:96–103. [PubMed: 20816784]

Grossman SD, Rosenberg LJ, Wrathall JR. 2001 Temporal–spatial pattern of acute neuronal and glial loss after spinal cord contusion. Exp Neurol 168:273–282. [PubMed: 11259115]

Ichiyama T, Okada K, Lipton JM, Matsubara T, Hayashi T, Furukawa S. 2000 Sodium valproate inhibits production of TNF-alpha and IL-6 and activation of NF-kappaB. Brain Res 857:246–251. [PubMed: 10700573]

Inoue K 2006 The function of microglia through purinergic receptors: neuropathic pain and cytokine release. Pharmacol Ther 109:210–226. [PubMed: 16169595]

Inoue K, Koizumi S, Tsuda M. 2007 The role of nucleotides in the neuron–glia communication responsible for the brain functions. J Neurochem 102:1447–1458. [PubMed: 17697046]

Jarvis MF. 2009 The neural–glial purinergic receptor ensemble in chronic pain states. Trends Neurosci 33:48–57. [PubMed: 19914722]

Jones TB, McDaniel EE, Popovich PG. 2005 Inflammatory-mediated injury and repair in the traumatically injured spinal cord. Curr Pharm Design 11:1223–1236.

Kerschensteiner M, Schwab ME, Lichtman JW, Misgeld T. 2005 In vivo imaging of axonal degeneration and regeneration in the injured spinal cord. Nat Med 11:572–577. [PubMed: 15821747]

Kim HJ, Rowe M, Ren M, Hong JS, Chen PS, Chuang DM. 2007 Histone deacetylase inhibitors exhibit anti-inflammatory and neuroprotective effects in a rat permanent ischemic model of stroke: multiple mechanisms of action. J Pharmacol Exp Ther 321:892–901. [PubMed: 17371805]

Kim HS, Whang SY, Woo MS, Park JS, Kim WK, Han IO. 2004 Sodium butyrate suppresses interferon-gamma-, but not lipopolysaccharide-mediated induction of nitric oxide and tumor necrosis factor-alpha in microglia. J Neuroimmunol 151:85–93. [PubMed: 15145607]

Lee JY, Kim HS, Choi HY, Oh TH, Ju BG, Yune TY. 2012 Valproic acid attenuates blood–spinal cord barrier disruption by inhibiting matrix metalloprotease-9 activity and improves functional recovery after spinal cord injury. J Neurochem 121:818–829. [PubMed: 22409448]

Li R, El-Mallahk RS. 2000 A novel evidence of different mechanisms of lithium and valproate neuroprotective action on human SY5Y neuroblastoma cells: caspase-3 dependency. Neurosci Lett 294:147–150. [PubMed: 11072136]

Li Y, Yuan Z, Liu B, Sailhamer EA, Shults C, Velmahos GC, Demoya M, Alam HB. 2008 Prevention of hypoxia-induced neuronal apoptosis through histone deacetylase inhibition. J Trauma 64:863–870; discussion 870–861. [PubMed: 18404049]

Loscher W 1978 Serum protein binding and pharmacokinetics of valproate in man, dog, rat and mouse. J Pharmacol Exp Ther 204:255–261. [PubMed: 340640]

Lv L, Han X, Sun Y, Wang X, Dong Q. 2011a Valproic acid improves locomotion in vivo after SCI and axonal growth of neurons in vitro. Exp Neurol 233:783–790. [PubMed: 22178331]

Lv L, Sun Y, Han X, Xu CC, Tang YP, Dong Q. 2011b Valproic acid improves outcome after rodent spinal cord injury: potential roles of histone deacetylase inhibition. Brain Res 1396:60–68. [PubMed: 21439269]

McCarthy KD, de Vellis J. 1980 Preparation of separate astroglial and oligodendroglial cell cultures from rat cerebral tissue. J Cell Biol 85:890–902. [PubMed: 6248568]

Mingam R, De Smedt V, Amedee T, Bluthe RM, Kelley KW, Dantzer R, Laye S. 2008 In vitro and in vivo evidence for a role of the $P2X_7$ receptor in the release of IL-1 beta in the murine brain. Brain Behav Immun 22:234–244. [PubMed: 17905568]

Monif M, Reid CA, Powell KL, Smart ML, Williams DA. 2009 The $P2X_7$ receptor drives microglial activation and proliferation: a trophic role for $P2X_7R$ pore. J Neurosci 29:3781–3791. [PubMed: 19321774]

Pan JZ, Ni L, Sodhi A, Aguanno A, Young W, Hart RP. 2002 Cytokine activity contributes to induction of inflammatory cytokine mRNAs in spinal cord following contusion. J Neurosci Res 68:315–322. [PubMed: 12111861]

Park JS, Woo MS, Kim SY, Kim WK, Kim HS. 2005 Repression of interferon-gamma-induced inducible nitric oxide synthase (iNOS) gene expression in microglia by sodium butyrate is mediated through specific inhibition of ERK signaling pathways. J Neuroimmunol 168:56–64. [PubMed: 16091294]

Penas C, Verdu E, Asensio-Pinilla E, Guzman-Lenis MS, Herrando-Grabulosa M, Navarro X, Casas C. 2011 Valproate reduces CHOP levels and preserves oligodendrocytes and axons after spinal cord injury. Neuroscience 178:33–44. [PubMed: 21241777]

Peng GS, Li G, Tzeng NS, Chen PS, Chuang DM, Hsu YD, Yang S, Hong JS. 2005 Valproate pretreatment protects dopaminergic neurons from LPS-induced neurotoxicity in rat primary midbrain cultures: role of microglia. Brain Res Mol Brain Res 134:162–169. [PubMed: 15790540]

Phiel CJ, Zhang F, Huang EY, Guenther MG, Lazar MA, Klein PS. 2001 Histone deacetylase is a direct target of valproic acid, a potent anticonvulsant, mood stabilizer, and teratogen. J Biol Chem 276:36734–36741. [PubMed: 11473107]

Schnell L, Fearn S, Klassen H, Schwab ME, Perry VH. 1999 Acute inflammatory responses to mechanical lesions in the CNS: differences between brain and spinal cord. Eur J Neurosci 11:3648–3658. [PubMed: 10564372]

Schwab JM, Guo L, Schluesener HJ. 2005 Spinal cord injury induces early and persistent lesional $P2X_4$ receptor expression. J Neuroimmunol 163:185–189. [PubMed: 15885321]

Song G, Cechvala C, Resnick DK, Dempsey RJ, Rao VL. 2001 Gene-Chip analysis after acute spinal cord injury in rat. J Neurochem 79:804–815. [PubMed: 11723173]

Trang T, Beggs S, Salter MW. 2006 Purinoceptors in microglia and neuropathic pain. Pflugers Arch 452:645–652. [PubMed: 16767466]

Trang T, Beggs S, Wan X, Salter MW. 2009 $P2X_4$-receptor-mediated synthesis and release of brain-derived neurotrophic factor in microglia is dependent on calcium and p38-mitogen-activated protein kinase activation. J Neurosci 29:3518–3528. [PubMed: 19295157]

Tsuda M, Shigemoto-Mogami Y, Koizumi S, Mizokoshi A, Kohsaka S, Salter MW, Inoue K. 2003 $P2X_4$ receptors induced in spinal microglia gate tactile allodynia after nerve injury. Nature 424:778–783. [PubMed: 12917686]

Tsuda M, Inoue K, Salter MW. 2005 Neuropathic pain and spinal microglia: a big problem from molecules in “small” glia. Trends Neurosci 28:101–107. [PubMed: 15667933]

Wang CY, Chen JK, Wu YT, Tsai MJ, Shyue SK, Yang CS, Tzeng SF. 2011 Reduction in antioxidant enzyme expression and sustained inflammation enhance tissue damage in the subacute phase of spinal cord contusive injury. J Biomed Sci 18:13. [PubMed: 21299884]

Wang X, Arcuino G, Takano T, Lin J, Peng WG, Wan P, Li P, Xu Q, Liu QS, Goldman SA, Nedergaard M. 2004 $P2X_7$ receptor inhibition improves recovery after spinal cord injury. Nat Med 10:821–827. [PubMed: 15258577]

Wang YC, Wu YT, Huang HY, Lin HI, Lo LW, Tzeng SF, Yang CS. 2008 Sustained intraspinal delivery of neurotrophic factor encapsulated in biodegradable nanoparticles following contusive spinal cord injury. Biomaterials 29:4546–4553. [PubMed: 18774604]

Xie N, Wang C, Lin Y, Li H, Chen L, Zhang T, Sun Y, Zhang Y, Yin D, Chi Z. 2010 The role of p38 MAPK in valproic acid induced microglia apoptosis. Neurosci Lett 482:51–56. [PubMed: 20621161]

Yu SH, Cho DC, Kim KT, Nam KH, Cho HJ, Sung JK. 2012 The neuroprotective effect of treatment of valproic Acid in acute spinal cord injury. J Korean Neurosurg Soc 51:191–198. [PubMed: 22737297]

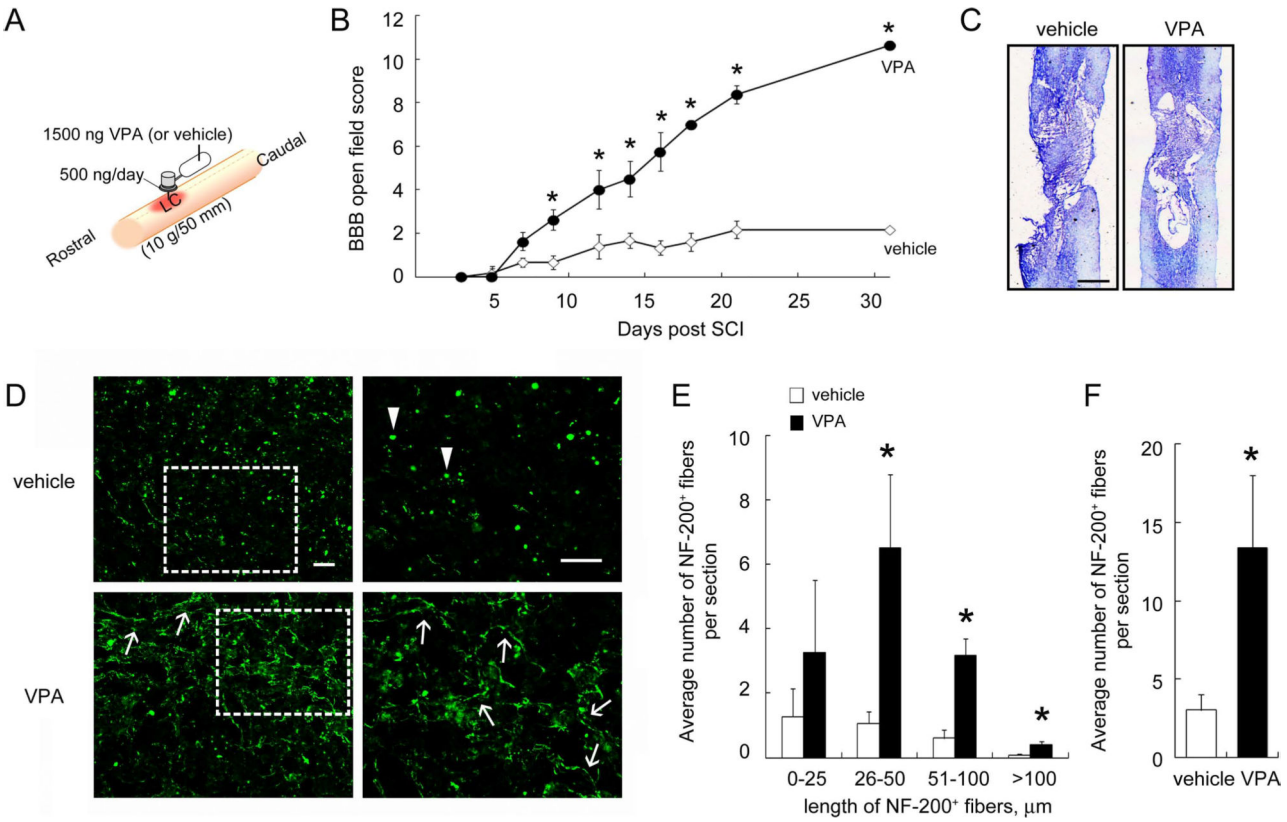

Fig. 1.

Improvement of hindlimb recovery in rats with SCI after intraspinal injection of VPA. **A:** Animals were subjected to contusive SCI and immediately treated by a 3-day infusion of VPA (500 ng/day) or vehicle (24 µl/day PBS) for 3 days via an osmotic pump implanted into the LC of the spinal cord immediately after contusive injury. The osmotic pump was removed at day 3 post-SCI. **B:** Hindlimb locomotor function was analyzed throughout the 31-day survival (n = 6 rats for vehicle; n = 8 rats for VPA) and indicated that VPA infusion improved hindlimb locomotor recovery in rats with SCI. **C:** The horizontal tissue sections were subjected to histological analysis as described in Materials and Methods. The representative stained tissue sections from the dorsal portion of the spinal cord indicated that the tissue loss of the vehicle-treated spinal cord was more severe than that observed in VPA-treated cord. **D:** Representative images of immunofluorescence for NF-200 were derived from the immunostained LC of the spinal dorsal portion (arrows). The higher magnification images shown at right were taken from the boxed areas at left. NF-200$^+$ neuronal fibers with different length (**E**), and the total number of NF-200$^+$ neuronal fibers observed at the LC were measured (**F**). The results are expressed as average number of NF-200$^+$ neuronal fibers measured in a field of 0.055 mm^2 (×400 area). Arrowheads in D indicate fragmented NF-200$^+$ neuronal debris. Scale bar = 1 mm in C; 50 µm in D. Data are presented as mean ± SEM. *P < 0.05 vs. relative vehicle at each time point (B) or vs. relative vehicle (E,F). [Color figure can be viewed in the online issue, which is available at wileyonlinelibrary.com.]

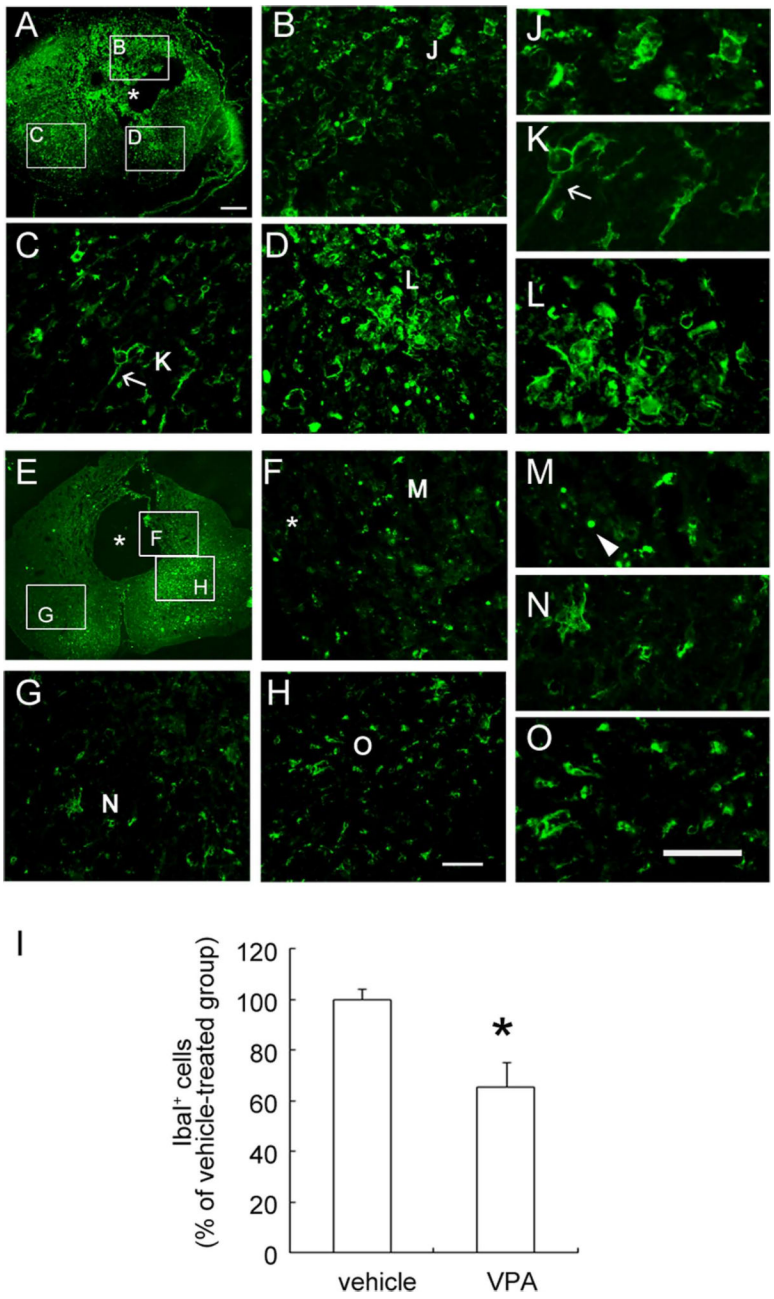

Fig. 2.

Immunofluorescence of Iba1 in the injured spinal cord. The cross-sections of the spinal cord collected at day 31 post-SCI 1–2 mm proximal to the epicenter were subjected to immunofluorescence for Iba1. Iba1$^+$ microglia/macrophages had accumulated in the lesion center (LC) of the vehicle-treated spinal cord (**A–D**). Most Iba1$^+$ microglia/macrophages in the LC displayed an amoeboid shape (**J,L**), and some cells showed a hypertrophic, ramified form (**K**, arrow). Fewer Iba1$^+$ microglia/macrophages were observed in the injured spinal cord of VPA-treated rats (**E–H,M–O**). Iba1$^+$ tissue debris was found in VPA-treated spinal cord tissue near the cavity (F, arrowhead in M). Many Iba1$^+$ cells displayed a hypertrophic morphology (G,H). Higher magnifications of the areas indicated in G and H are shown in N

and O. Iba1$^+$ microglia observed in these regions were quantified (**I**). Data shown in I are presented as mean ± SEM and are expressed as Iba1$^+$ cells per cross-section (n = 3 rats). *P < 0.05 vs. vehicle. Asterisks in A, E, and F indicate the tissue cavity. Scale bars = 200 μm in A (applies to A,E); 50 μm in H (applies to B–D,F–H); 50 μm in O (applies to J–O). [Color figure can be viewed in the online issue, which is available at wileyonlinelibrary.com.]

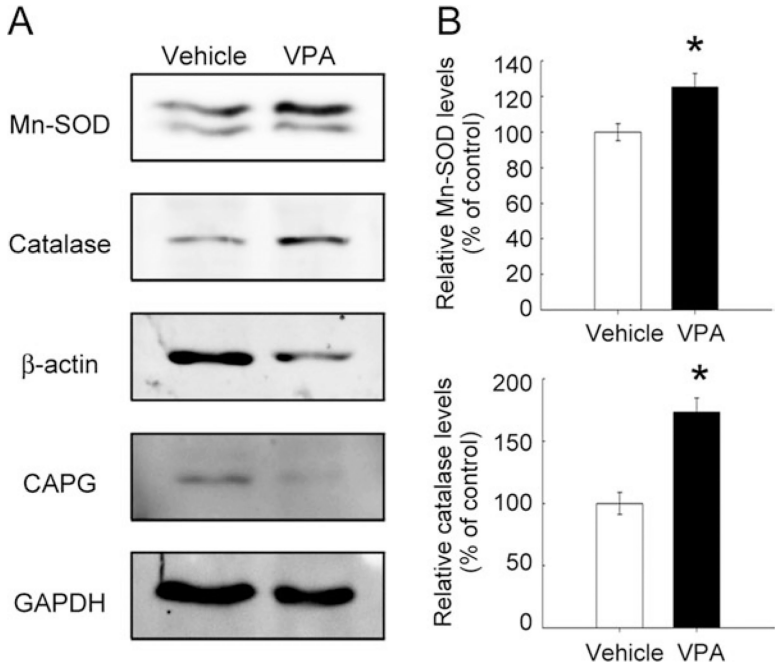

Fig. 3.

Expression of Mn-SOD and catalase in the lesion center of the spinal cord receiving VPA infusion. **A:** Proteins were extracted from the LC of the spinal cord at the indicated survival times after severe SCI, then subjected to Western blot analysis for the expression of β-actin and CAPG. **B:** Proteins were extracted from the LC of the injured spinal cords at day 7 post-SCI and then examined by Western blot analysis for Mn-SOD, catalase, β-actin, and CAPG protein levels. The relative intensity of Mn-SOD and catalase protein levels normalized to GAPDH was measured. Data are presented as mean ± SEM of percentage of the vehicle-treated control from three separate experiments. $*P < 0.05$ vs. vehicle.

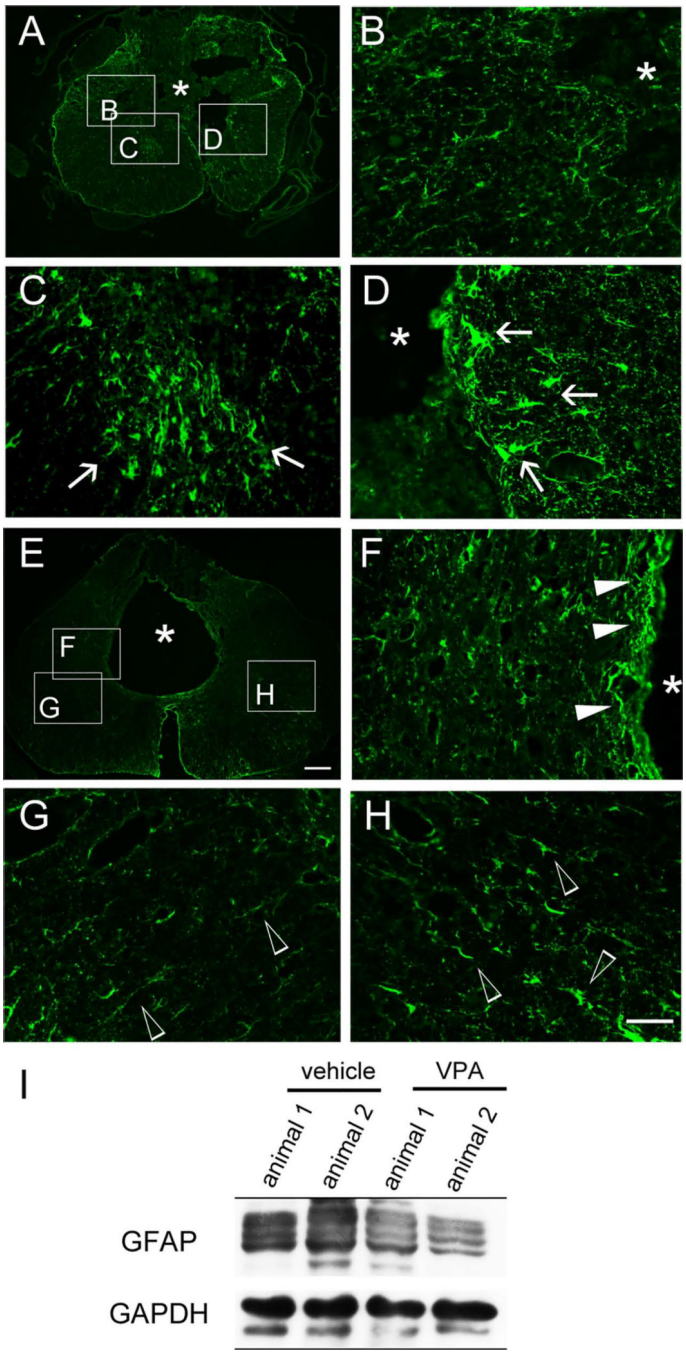

Fig. 4.

Immunofluorescence of GFAP in the injured spinal cord tissues. The spinal cord cross-sections collected from vehicle-treated (**A–D**) and VPA-infused (**E–H**) rats at day 31 post-SCI were subjected to immunofluorescence for GFAP. Hypertrophic astroyctes with intense GFAP staining were observed in the LC of vehicle-treated spinal cord (arrows in C,D), whereas cells with less intense GFAP staining were also found in some regions of the injured spinal cord section (B). In addition, $GFAP^{+}$ astrocytes were present in the penumbra around the tissue cavity of VPA-treated spinal cord (F, solid arrowheads), whereas

hypotrophic GFAP$^+$ astrocytes were scattered in the regions of the injured spinal cord sections (G,H, open arrowheads). To examine the levels of GFAP in the injured spinal cord tissues, the spinal tissues containing the LC regions were collected from vehicle- and VPA-treated rats at day 31 post-SCI and then subjected to Western blot analysis (**I**). Asterisks in A,B,D–F indicate the injured cavity of the cord. Scale bar = 200 μm in E (applies to A,E); 50 μm in H (applies to B–D,F–H). [Color figure can be viewed in the online issue, which is available at wileyonlinelibrary.com.]

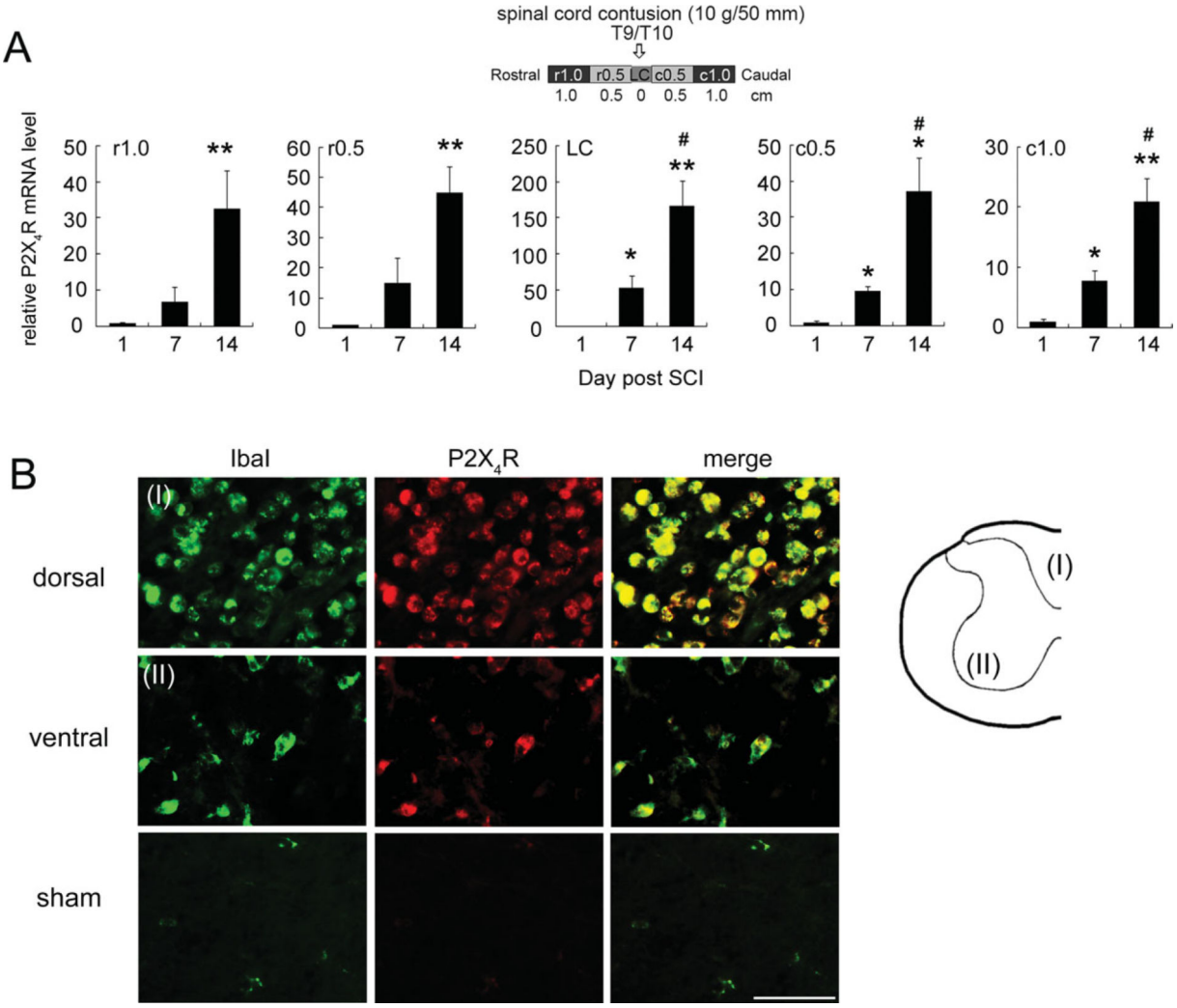

Fig. 5.

Temporal and spatial expression of $P2X_4R$ mRNA in the injured spinal cord. **A:** RNA samples were prepared from spinal cord tissues rostral (r0.5 and r1) and caudal (c0.5 and c1) to the injury center (LC) at days 1, 7, and 14 postcontusive injury to T9/T10. $P2X_4R$ mRNA levels in each spinal cord region were determined by Q-PCR. Data are shown as mean ± SEM (n = 3 rats for each time point) and are expressed as relative expression of $P2X_4R$ mRNA levels in each injured cord section compared with that detected at day 1 post-SCI. $^{*}P < 0.05$, $^{**}P < 0.01$compared with the group at day 1 post-SCI; $^{\#}P < 0.05$ compared with the group at day 7 post-SCI. **B:** Spinal cord tissues were collected from the LC of the injured spinal cord at day 7 from SCI rats. The spinal cord cross-sections were subjected to double immunofluorescence for $P2X_4R$-and IbaI-expressing microglia/macrophages, which had greatly accumulated in the cavity of the dorsal portion (I). In addition, amoeboid $P2X_4R^+$/$IbaI^+$ microglia/macrophages were scattered in the remaining injured tissue of the ventral portion (II). The representative images indicate that rare detectable levels of $P2X_4R^+$/$IbaI^+$ microglia/macrophages were found in the sham-operated spinal cord tissue. Scale bar = 50 μm.

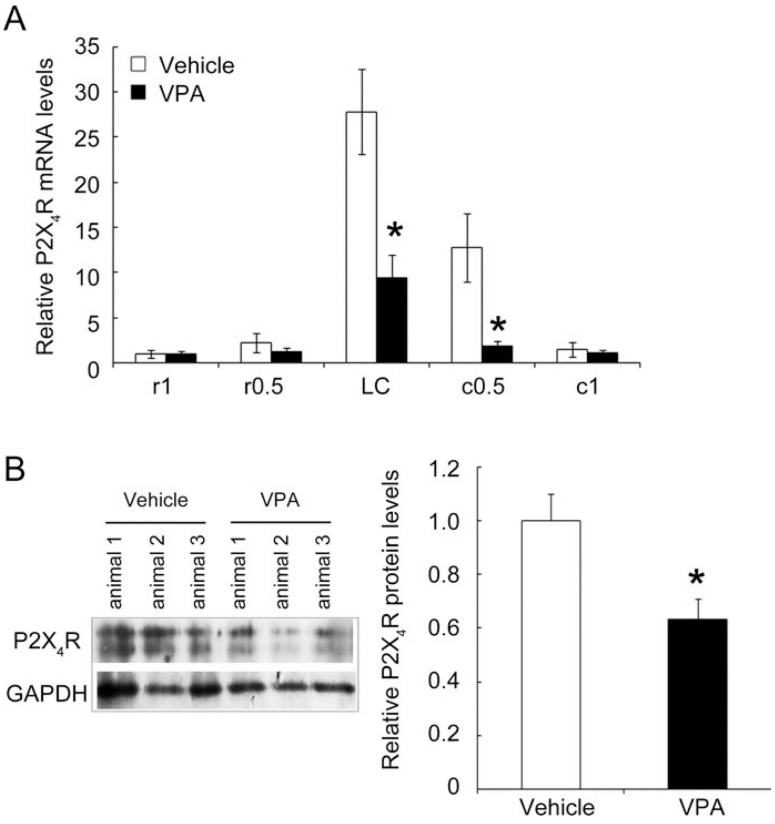

Fig. 6.

Comparative examination of $P2X_4R$ mRNA levels in the injured spinal cord of rats receiving infusion with vehicle or VPA. After SCI, animals received infusion with vehicle (24 μl of PBS per day) or with VPA (500 ng per day) for 3 days using an osmotic pump. **A:** Total RNA samples were prepared from spinal cord tissues rostral (r0.5 and r1) and caudal (c0.5 and c1) to the LC at day 14 post-SCI. $P2X_4R$ mRNA levels in each spinal cord region were determined by Q-PCR. Data are shown as mean ± SEM (n = 3 rats for vehicle- or VPA-treated group) and are expressed as relative expression of $P2X_4R$ mRNA levels in each injured cord section compared with that detected in r1 of the vehicle-treated group. **B:** Alternatively, total proteins were prepared from the LC of the vehicle- or VPA-treated spinal cord at day 7 post-SCI and then subjected to Western blotting to measure the levels of $P2X_4R$ proteins. $*P < 0.05$ compared with the analogous spinal portion from the corresponding vehicle-operated group.

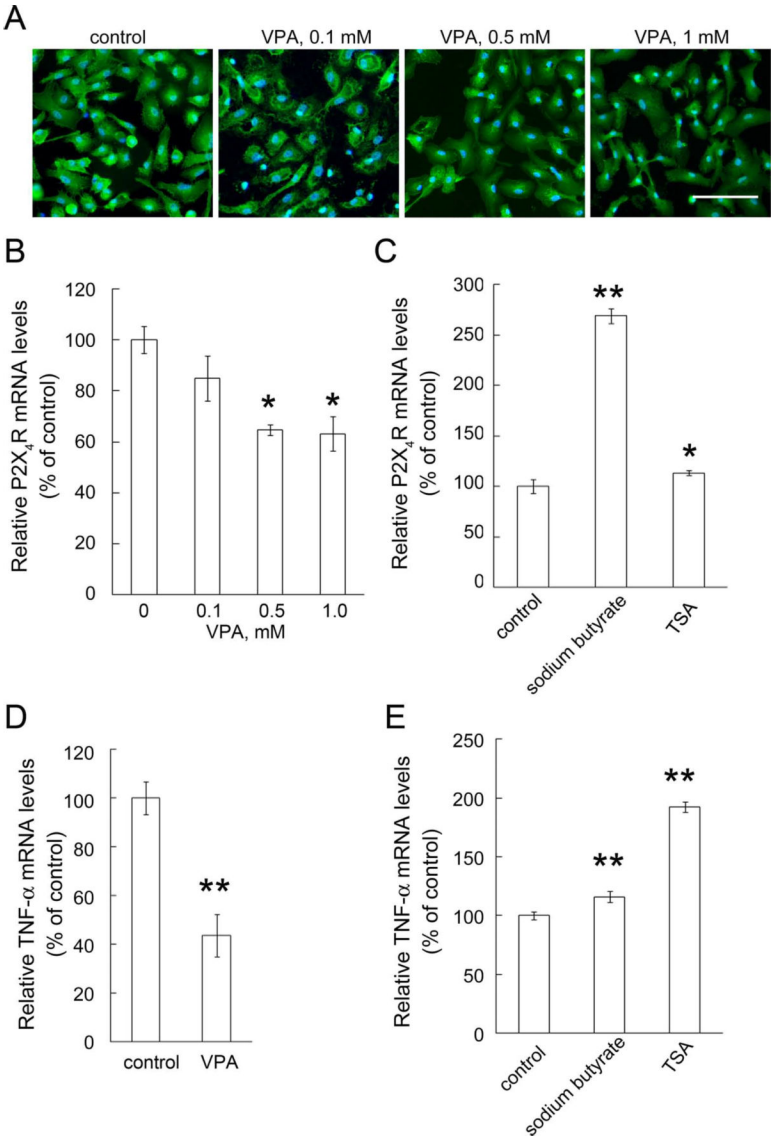

Fig. 7.

Decreased expression levels of $P2X_4R$ and TNF-α by VPA in LPS-activated microglia. **A:** Primary microglia were stimulated with LPS (10 ng/ml) for 6 hr and then treated with VPA at the indicated concentrations for another 18 hr in the presence of LPS. The cultures were subjected to IbaI immunofluorescence staining. **B:** VPA at the indicated concentrations was added to the cultures after stimulation with 10 ng/ml of LPS for another 18 hr. **C**: Primary microglia were treated with sodium butyrate (1 mM) and TSA (100 nM) for 18 hr after stimulation with 10 ng/ml of LPS for 6 hr. The cultures (B,C) were then subjected to Q-PCR for the measurement of the mRNA levels of $P2X_4R$ (B,C) and TNF-α (**D,E**). $P2X_4R$ or TNF-α mRNA levels were normalized to the levels of CyPA. Data are presented as mean ± SEM of percentage of LPS-treated control from at least three separate experiments. $*P < 0.05$, $**P < 0.0$ vs. respective vehicle-treated control. Scale bar = 100 μm. [Color figure can be viewed in the online issue, which is available at wileyonlinelibrary.com.]

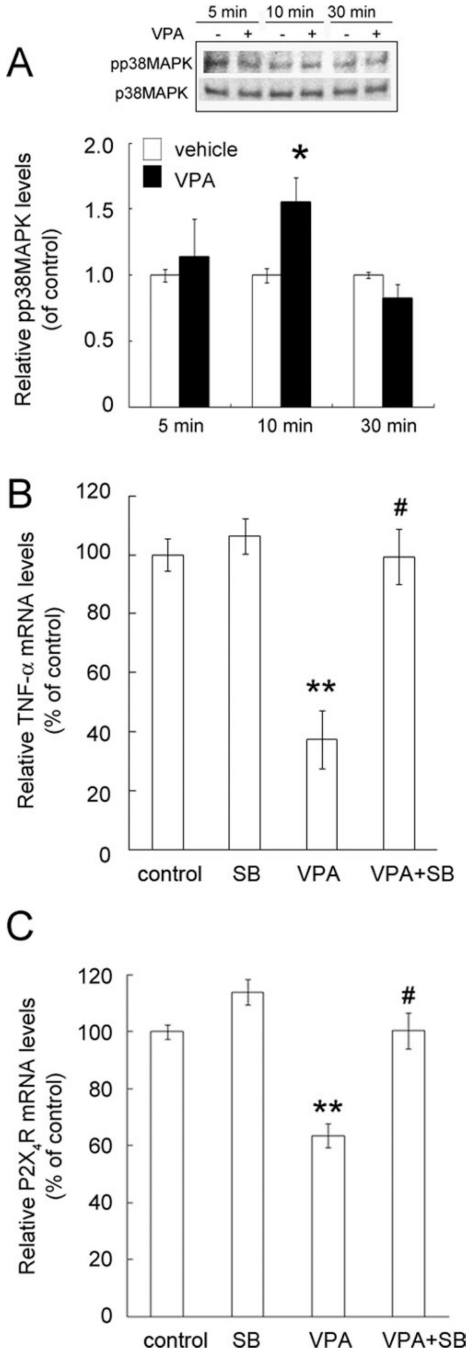

Fig. 8.

Blockade of VPA effect on the downregulation of P2X4R expression by the p38MAPK inhibitor SB203580. **A:** Primary microglia were stimulated with LPS (10 ng/ml) for 6 hr and then exposed to 1 mM of VPA for 5, 10, and 30 min. The phosphorylation of p38MAPK was examined by Western blot analysis. The equal expression level of total p38MAPK was used as a loading control, and the experiments were repeated at least three times. The levels of phosphorylated p38MAPK (pp38) and total p38MAPK on immunoblots were quantified by densitometry. **B,C:** Microglia were activated with 10 ng/ml LPS for 6 hr. Before exposure to

1 mM VPA for 18 hr, LPS-stimulated microglia were pretreated with 1 μM SB203580 (SB) for 30 min. The cultures were then subjected to Q-PCR analysis for the measurement of TNF-α (B) and P2X4R (C) mRNA levels. TNF-α and P2X4R mRNA levels were normalized to levels of CyPA. Data are presented as mean 6 SEM of percentage of LPS-treated control from three separate experiments. $*P < 0.05$, $**P < 0.01$ vs. control; $\#P < 0.01$ vs. VPA-treated group.